JOURNAL OF MATERIALS SCIENCE 32 (1997) 2403–2409

Crystalline and quasicrystalline phases in AlCuFe and AlCuFeCr alloys

G. ROSAS
Instituto de Investigaciones Metalúrgicas, UMSNH, P O. Box 52-B, 58000 Morelia Michoacán, México

R. PÉREZ*
Instituto Nacional de Investigaciones Nucleares, Km 36.5, Carretera, Mexico Tduca, 52045 Salazar, México

Different chemical compositions of the AlCuFe and the AlCuFeCr systems have been studied. The liquid melts have been cast in different mould types where the rate of cooling can be varied. The experimental results showed that for slow solidification rates and in the case of the ternary alloys, binary compounds can only be obtained. However, for higher cooling velocities, binary, ternary and quasicrystalline compounds were obtained. In the quaternary case, higher cooling velocities produce an amorphization tendency in the obtained alloy. But for slow rates of cooling, binary, ternary and quasicrystalline compounds were obtained. High rates of cooling in the ternary alloys produce a microstructure with a high density of star-shaped dendrites. Some of these dendritic formations display apparent ten-fold rotational symmetry.

1. Introduction

During recent years, a large number of investigations related to alloys of AlCuFe and AlCuFeCr have been carried out [1–5]. This recent interest has been mainly prompted due to the finding of quasicrystalline phases in these types of alloys when they are cast under conventional solidification techniques. Thus, for example, Gayle *et al.* [6] carried out a complete study of the AlCuFe equilibrium phase diagram which includes 0–25 at % Fe and 50–75 at % Al. One of the main objectives of this study was to obtain the structural relationships between the icosahedral phase and all the other stable phases. The icosahedral phase in the AlCuFe system has been found to be very sensitive to the chemical composition of the alloy [4, 6]. However, there are very few investigations in the literature [5] related to the microstructural characteristics of the AlCuFe compounds for chemical compositions close to the alloy initially reported by Tsai *et al.* [1]. This ternary composition is important because the icosahedral phase was initially found in this type of compound. The interest also in this region of the ternary phase diagram is related to the different crystalline structures [7–9] which have recently been obtained together with the icosahedral phase. Quasicrystalline phases in the ternary system of AlCuCr have also been reported [5]. However, there are very few reports on the study of the quasicrystalline phases for the quaternary alloys of the AlCuFeCr system [5]. On the other hand, the formation of the quasicrystalline phases in the AlCuFe and AlCuCr systems have been found to be very sensitive to the rate of cooling from the liquid melt.

The results reported in this investigation are related to the microstructural characterization of the quasicrystalline and crystalline phases obtained in ternary alloys of the AlCuFe system. The chemical compositions have been set closely to the composition initially reported by Tsai [1], where the icosahedral phase has been firstly obtained. The liquid melt has been cast in two different moulds: a V-shaped mould where different rates of cooling can be obtained along the wedge shaped ingot and a normal cylindrical mould. Also, a microstructural characterization has been carried out for the crystalline and quasicrystalline phases in quaternary alloys of the AlCuFeCr system. These alloys have been cast in the same type of moulds used for the ternary alloys.

2. Experimental procedure

The alloys were prepared with 150 g loads of high purity (99.99%) aluminium, copper and iron. These elements were put in a graphite crucible and melted using an induction furnace of approximately 10 kVA. The liquid melt was always under an inert atmosphere of argon. When the liquid melt was at a temperature of approximately 1500° C, the alloy was cast into two differents moulds. A cylindrical cavity in a piece of stainless steel was used as one of the moulds. The other mould used was the wedge cavity made with two polished copper plates. The average chemical

*On leave from the Laboratorio de Cuernavaca, Instituto de Física UNAM, P.O. Box 48-3, 62251 Cuernavaca Mor, Mexico

0022–2461

TABLE I Compositions of the alloy systems

No.	Nominal compositions	Chemical analysis AAE
1	$Al_{65}Cu_{20}Fe_{15}$	$Al_{64.8}Cu_{20}Fe_{15.2}$
2	$Al_{60}Cu_{28}Fe_{12}$	$Al_{60.2}Cu_{27.8}Fe_{12}$
3	$Al_{62}Cu_{28}Fe_{10}$	$Al_{62.2}Cu_{27.8}Fe_{10}$
4	$Al_{65}Fe_{15}Cu_{10}Cr_{10}$	$Al_{64.7}Fe_{15.2}Cu_{10}Cr_{10.1}$

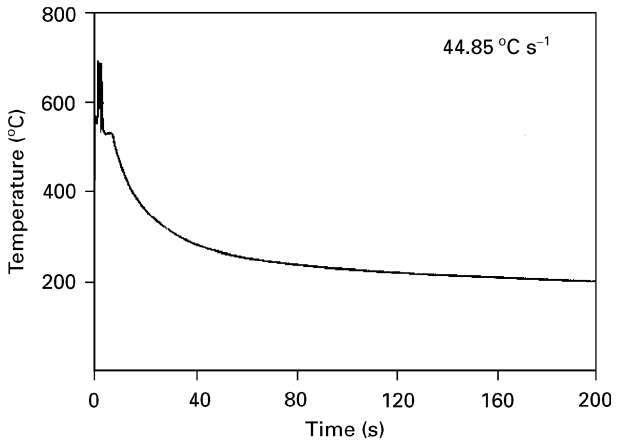

Figure 1 Rate of cooling for the wedge ingot. This plot corresponds to the thin region.

composition of the produced ingots was obtained with an atomic absorption spectroscopy method. The prepared alloys and their corresponding nominal compositions are displayed in Table I.

The obtained ingots were cut along the transverse and longitudinal sections. The cut sections were subsequently used for the microstructural characterization based on optical microscopy, scanning electron microscopy and microanalysis. Initially they were mechanically polished using different types of grinding paper from 200 up to 1000 μm and the final polishing step was carried out using a diamond compound abrasive. The specimens for the transmision electron microscope observations were also initially mechanically polished. However, the final polishing method employed an electrochemical approach using an electrolyte made of 67% methanol and 33% HNO_3.

Powders from different regions in the specimens were obtained and subsequently used for the X-ray diffraction studies. The cooling rates of the different alloys in the top, medium and bottom sections of the wedge ingots were obtained. In addition, this rate was obtained in the medium sections of the cylindrical ingot. In order to obtain these rates, chromel–alumel thermocouples and a small personal computer to record and plot the data, were used (Fig. 1). The instruments used in the microstructural characterization of these alloys were mainly an optical microscope Olimpus PGM3, a scanning electron microscope JSM-6400 with EDS attachments, a Phillips X-ray diffractometer, a Perkin–Elmer atomic absorption spectrometer and a transmission electron microscope Jeol-100CX.

3. Results and discussion

3.1. AlCuFe system

The alloy of composition 1, as indicated in Table I is similar to the alloy first reported by Tsai [1]. He

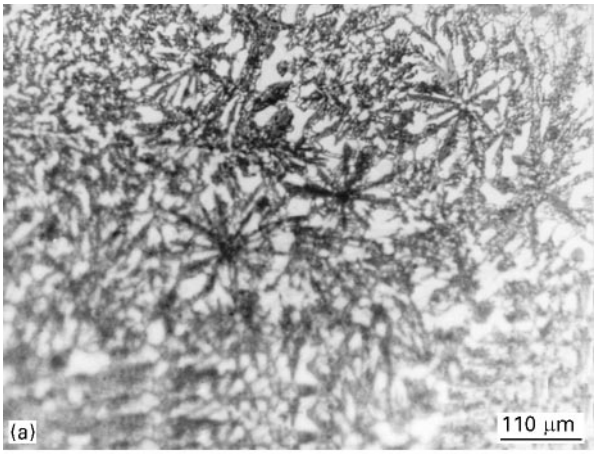

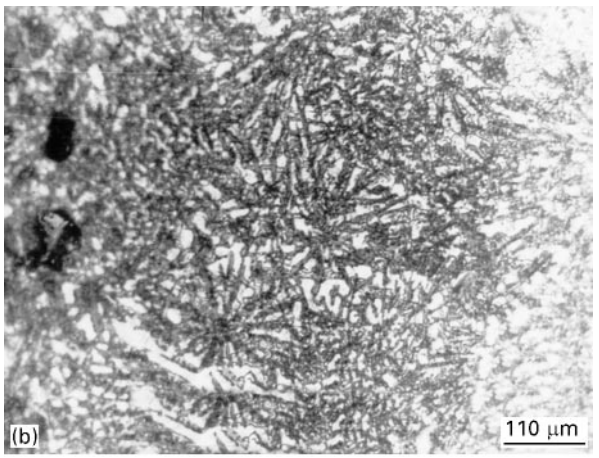

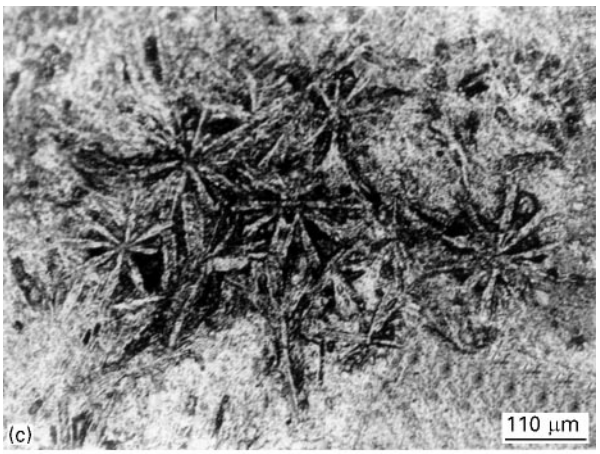

Figure 2 (a, b) Optical microscope images from the wedge specimen ($Al_{65}Cu_{20}Fe_{15}$) corresponding to the inner surface of the thin region of the wedge (approximately 2 mm under the normal surface). (c) This image was obtained from the specimen surface which has been in contact with the copper mould surface.

reported the presence of a quasicrystalline phase in this compound. This phase corresponds to an icosahedral phase. The microstructure obtained from alloy 1 in the bottom section of the wedge-shaped ingot is illustrated in Fig. 2. In this figure, there are clear indications of dendritic formations with apparent ten-fold symmetry. These regions also correspond to the areas where the highest cooling rates ($44.85^{\circ}C\,s^{-1}$) were obtained (Fig. 1). It is interesting to point out that these dendritic formations are not

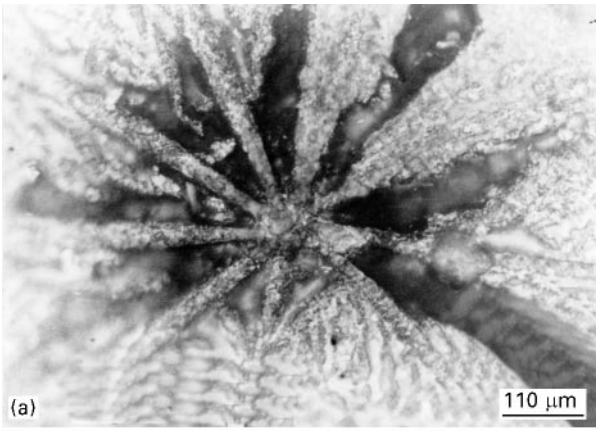

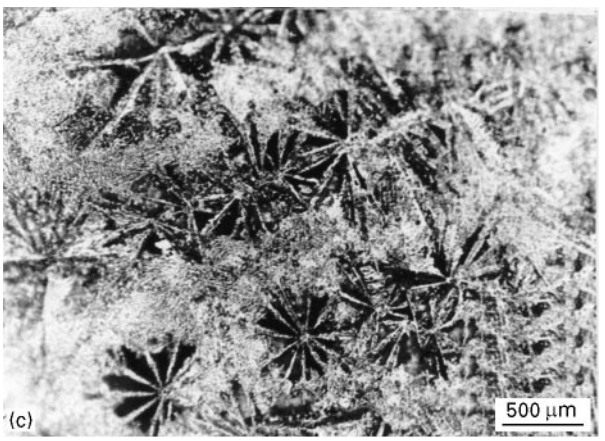

Figure 3 Characteristic microstructure in the thin regions of the wedge-shaped ingot from alloy ($Al_{60.2}Cu_{27.8}Fe_{12}$) (a–c) correspond to different views of the star-shaped dendrites.

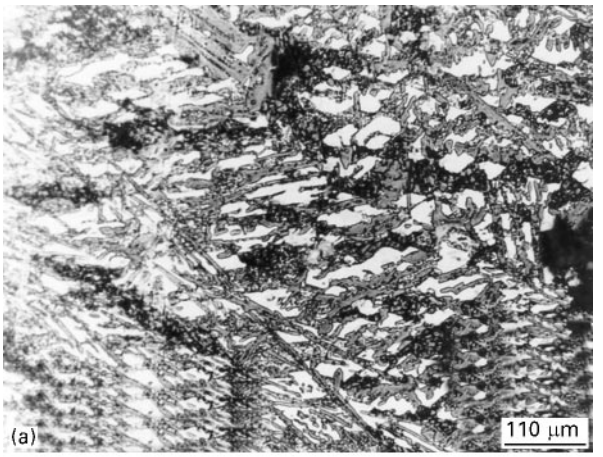

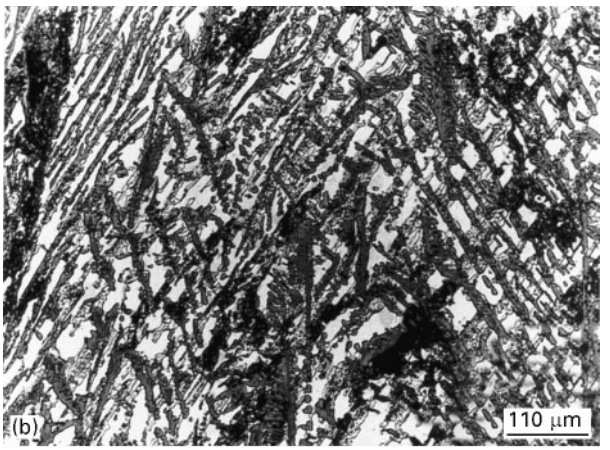

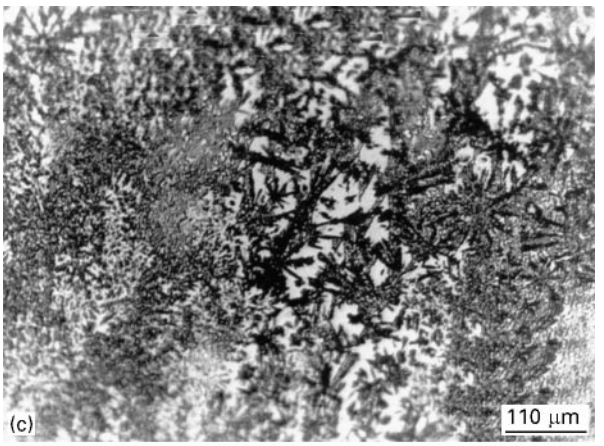

Figure 4 Optical micrographs from different regions in the wedge ingot from alloy ($Al_{62.2}Cu_{27.8}Fe_{10}$). (a) thick region, (b) medium region, and (c) thin region.

only on the ingot surface which is in contact with the wedge-shaped mould, but also in inner regions (2 mm thick) of the same specimen as is illustrated in Fig. 2. The dendritic character of the quasicrystalline phases has been reported in the past for different alloys [5, 10]. In these reports, the nucleus of these dendritic formations has been suggested to be of quasicrystalline nature and the arms usually of intermetallic nature. These types of dendrite have been found in the thin areas of the wedge ingot for the three alloy compositions. Thus, for example, Fig. 3 shows these formations for the alloys compositions 2. Fig. 4 shows the optical micrographs obtained from the top, medium and bottom regions of the wedge ingot for the alloy composition 3. These regions correspond to three different cooling rates ($24.3^\circ C\,s^{-1}$ in the thick section, $32.3^\circ C\,s^{-1}$ in the middle section and $44.85^\circ C\,s^{-1}$ in the thin section) (Fig. 1). Fig. 4a and b illustrate the formation of binary phases (compounds) which have been identified as Al_2Cu, Al_3Fe in an α-Al matrix; also there are traces of the ternary compound Al_7Cu_2Fe. These compounds have been identified through X-ray diffraction patterns, as will be discussed in the next paragraph. It is important to notice that in the thin regions of the wedge ingot there are clear indications of the dendritic formations with ten-fold apparent symmetries. On the other hand,

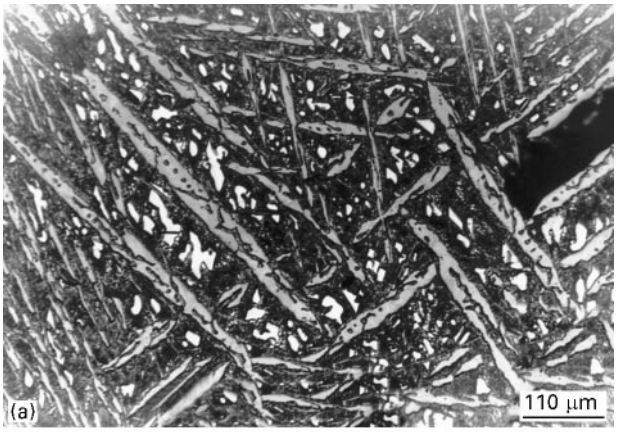

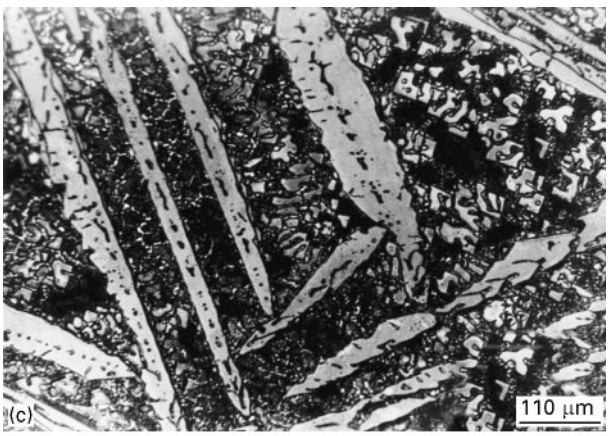

Figure 5 Optical characteristic microstructure from alloy 3 ($Al_{62.2}Cu_{27.8}Fe_{10}$) cast in the cylindrical mould. The three images (a, b and c) correspond to the obtained microstructure in three different regions along the main axis of the cylindrical ingot.

Fig. 5 shows the microstructure obtained in three different regions of the cylindrical ingot for the alloy 3. There are clear similarities between the microstructure in this cylindrical ingot and those microstructures obtained in the thick regions of the wedge ingot, mainly binary compounds in an α-Al matrix. Fig. 6 illustrates some of the morphological details of the dendrites with an apparent ten-fold symmetry which have been obtained in the thin sections of the wedge ingot in the AlCuFe alloys. It has been reported in the past that the nucleus of these dendritic formations has a composition close to $Al_{65}Cu_{20}Fe_{15}$ [4]. For example, Bradley and Goldschmidt [11] reported

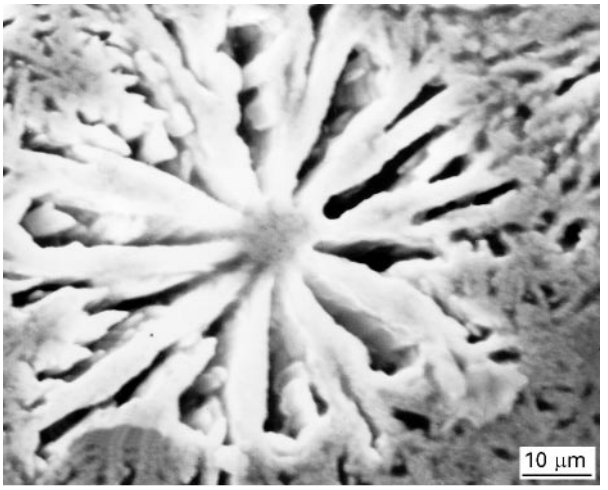

Figure 6 Scanning electron micrograph of a star-shape dendrite with an apparent ten-fold symmetry ($Al_{65}Cu_{20}Fe_{15}$).

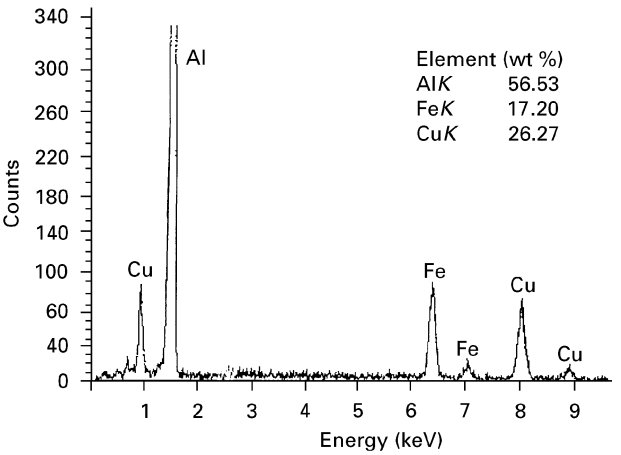

Figure 7 EDS microanalysis obtained from the central region of a dendrite. The area from where this composition pattern has been obtained has an appreciable density of star-shaped dendrites.

that the composition values where the icosahedral phase (so called ψ phase) is obtained, are in the ranges of 20%–26% Cu and 12–13.5% Fe. Therefore, the nucleus of the dendritic formations which are closely related to the quasicrystalline phase, should be rich in iron. This experimental result is also obtained from the dendrites in the thin sections of the wedge. This is illustrated in Fig. 7 where an EDS spectrum obtained from the central region of a dendrite, indicates an appreciable amount of iron compared with other regions in the specimen. Furthermore, the three ternary alloys were obtained under similar solidification conditions (wedge shape). However, the ternary alloy with larger contents of iron, shows a strong tendency for the dendritic formation with apparent ten-fold symmetry.

Fig. 8, on the other hand, shows details of the binary alloys obtained in the cylindrical mould from the alloy 3. These images have been obtained with the scanning electron microscope. The microstructure is similar to the microstructure obtained in the thick regions of the wedge-shaped ingot.

X-ray diffraction patterns have been obtained from the wedge ingots in the thick and thin regions. Fig. 9

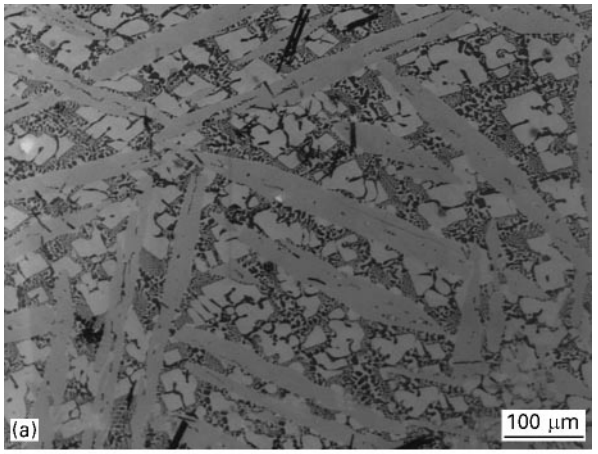

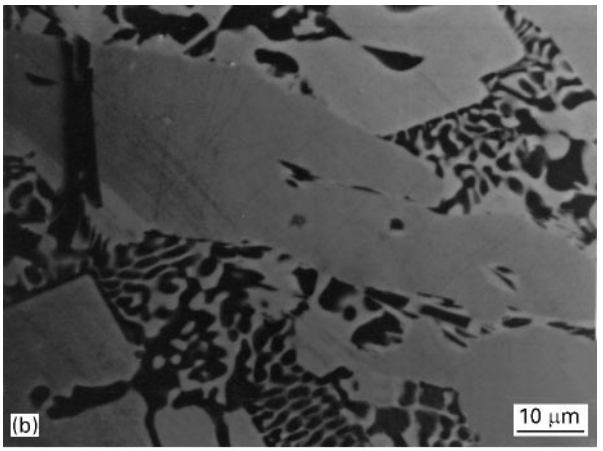

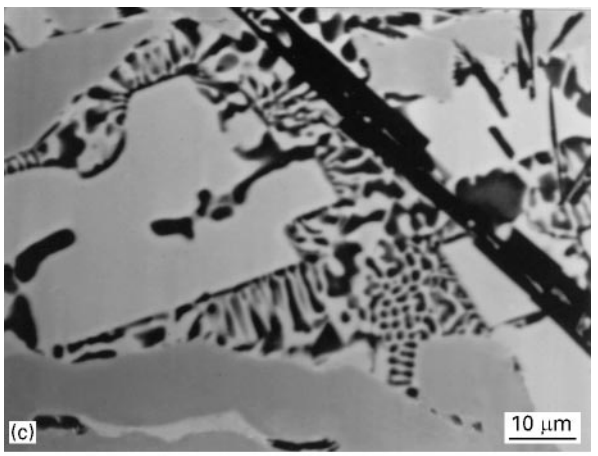

Figure 8 SEM images of the microstructure obtained from alloy 3 ($Al_{62.2}Cu_{27.8}Fe_{10}$) cast in the cylindrical mould. The three images (a, b and c) correspond to different sections along the main axis of the cylindrical ingot.

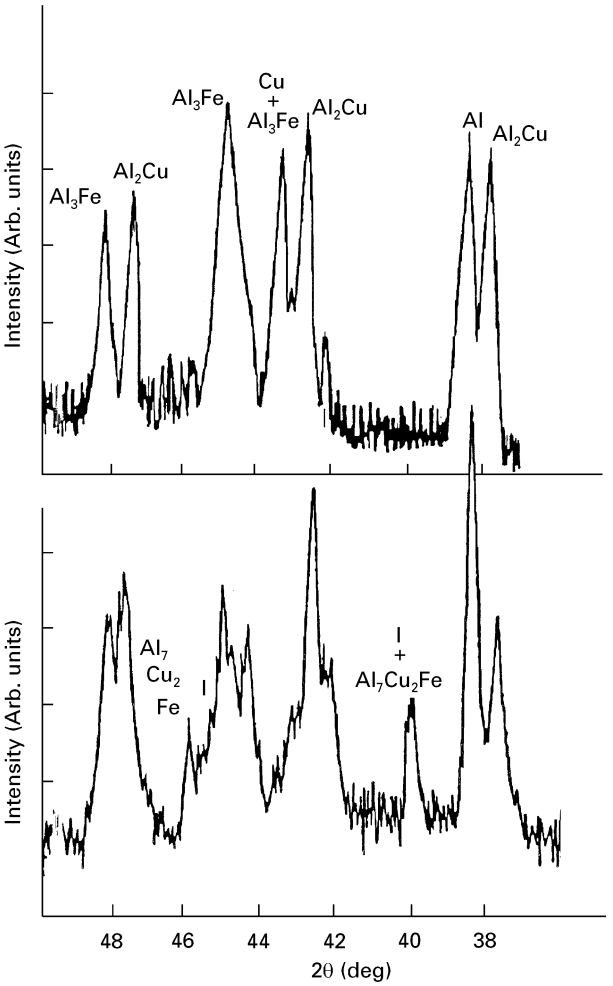

Figure 9 X-ray diffraction patterns from two different regions in the wedge-shaped ingot from alloy 2 ($Al_{60.2}Cu_{27.8}Fe_{12}$). The top spectrum corresponds to the thick region of the wedge and the bottom spectrum to the thin region of the wedge.

shows the X-ray spectrum from the alloy 2. In the thick section of the wedge (top spectrum) the binary compounds have been identified; however, in the thin section (bottom spectrum) the ternary compound Al_7Cu_2Fe and some peaks which correspond to the icosahedral phase have been obtained. Similar X-ray diffraction results have been obtained from the wedge ingots of alloy 3 and are illustrated in Fig. 10.

Finally, electron diffraction patterns have been obtained from the different ternary alloys. The icosahedral phase has been identified by obtaining the diffraction patterns from the most common quasicrystalline orientations, mainly the five-, three- and two-fold orientations. These are illustrated in Fig. 11, which shows electron diffraction patterns obtained from the icosahedral phase in the alloy 1.

3.2. AlCuFeCr system

The characteristic microstructure of a wedge-shaped ingot of the quaternary alloy (4) is illustrated in Fig. 12. These optical micrographs correspond to the thick, medium and thin regions of the wedge. In the thick and medium regions there are clear indications of the equilibrium phase formation. In these regions, some of the phases can be identified as Al_2Cu, Al_7Cu_2Fe and α-Al. However, in the thin regions, the identification of the phases is difficult because of the amorphization tendency of the alloy. This is clearer from Fig. 13, where the X-ray diffraction patterns from the thick, medium and bottom regions of the wedge specimen are shown. In the thick regions (top spectrum), the binary and ternary compounds

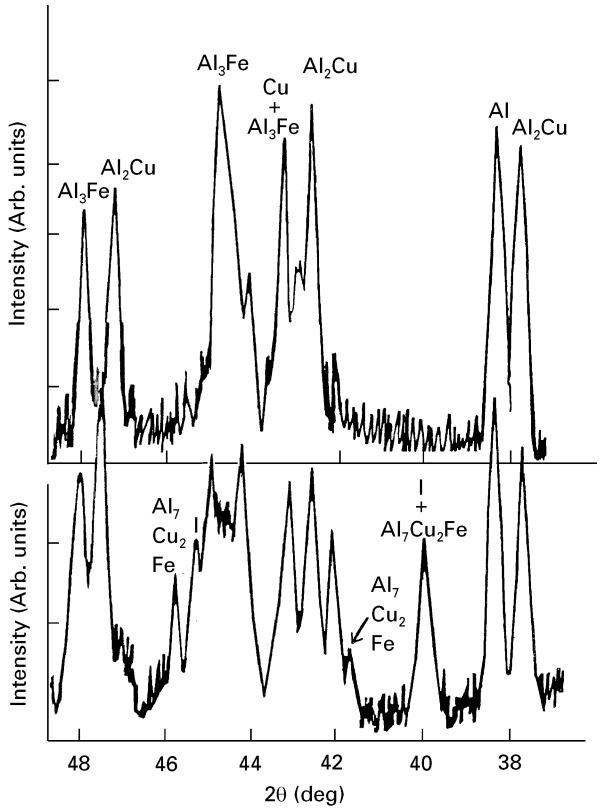

Figure 10 X-ray diffraction patterns from two different regions in the wedge-shaped ingot from alloy 3 ($Al_{62.2}Cu_{27.8}Fe_{10}$). The top spectrum corresponds to the thick region of the wedge and the bottom spectrum to the thin region of the wedge.

have been identified; however, in the thin regions the X-ray spectrum (bottom spectrum) shows clear indications of an amorphization phenomenon. In the top spectrum there are also some peaks which correspond to the icosahedral phase of the binary alloy $AlCr_{14}$.

4. Conclusions

The experimental results illustrated in this investigation show that for slow solidification rates, binary compounds are obtained in the ternary alloys of the AlCuFe system. However, along the edge of the wedge ingot, where the solidification rates are higher, ternary compounds and also quasicrystalline phases are commonly obtained. For the quaternary alloy of the AlCuFeCr system, there is a tendency for the amorphization to occur in the thin regions of the wedge ingot. This region corresponds to the higher cooling rates. However, in the thick region of the wedge, binary and ternary compounds have been obtained, in addition to some peaks which can be associated with the quasicrystalline phase in the $AlCr_{14}$ compound. A thermodynamical analysis for the alloy systems which has been presented here, based on recent reported values of ΔH in the solid state [12] predicts relationships of attraction and repulsion between the possible alloyed elements in the binary compounds. Thus, for example, in the AlCuFe, both binary phases AlFe and AlCu have the same probabilities for being formed. This effect is clearly shown in the X-ray diffraction pattern obtained from the ternary AlCuFe alloy. In the quaternary alloy AlCuFeCr, the binary compounds AlCu, AlFe and AlCr have values of ΔH which indicate strong attractions between the alloyed elements Therefore, these types of phase are more commonly obtained in the X-ray diffraction patterns. A complete thermodynamical study of the behaviour of these types of alloy will be the object of a future publication.

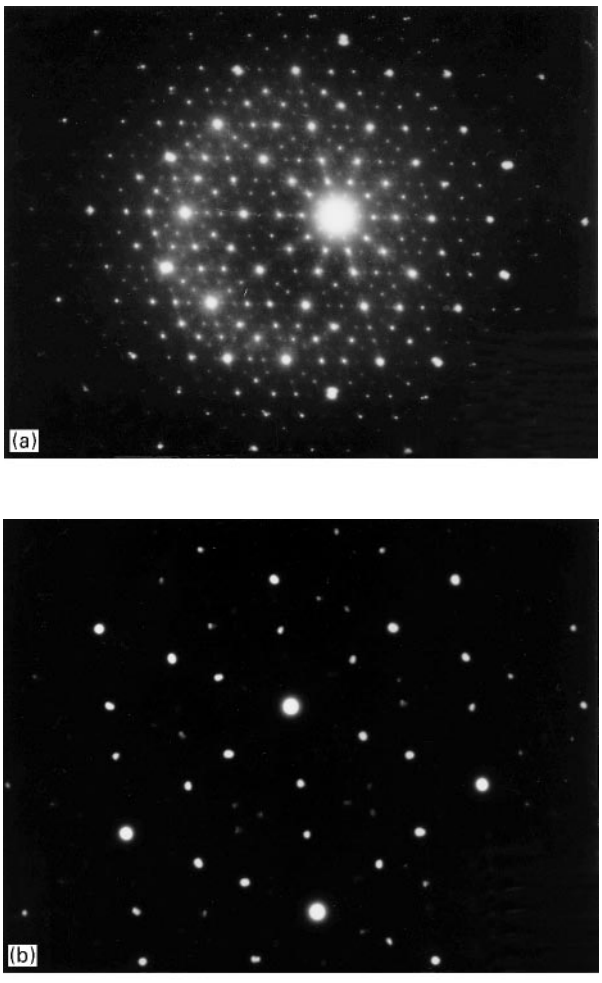

Figure 11 Electron diffraction patterns from the icosahedral phase in alloy 1: (a) five-fold, (b) three-fold, and (c) two-fold.

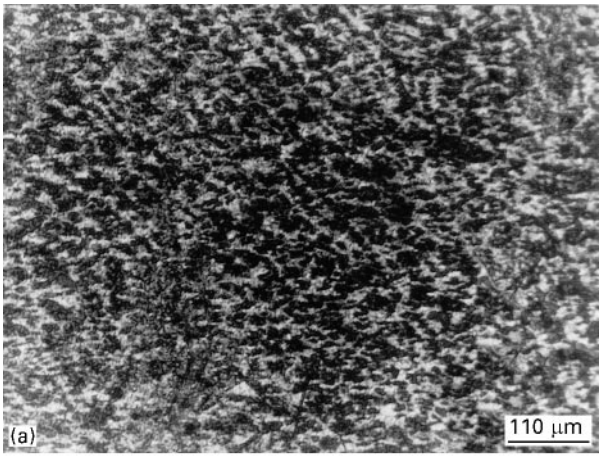

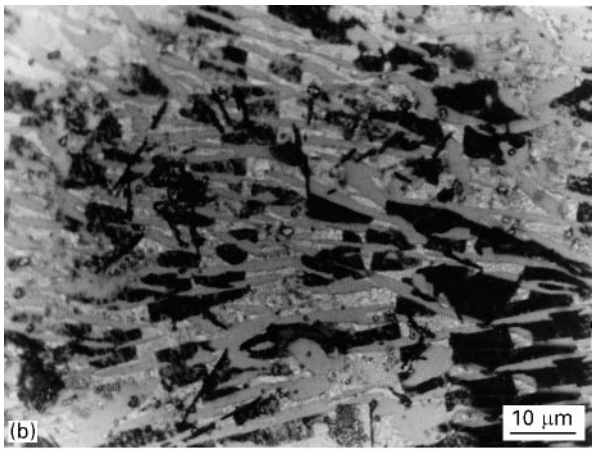

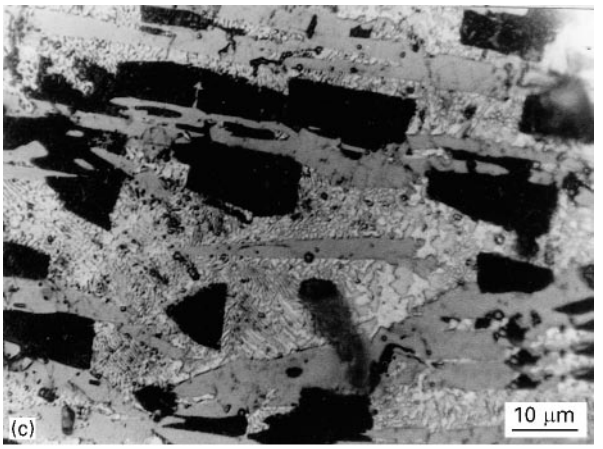

Figure 12 Microstructural characteristics of the quaternary alloy (4) cast in a wedge-shaped mould: (a) thin region of the wedge, (b) medium region of the wedge, and (c) thick region of the wedge.

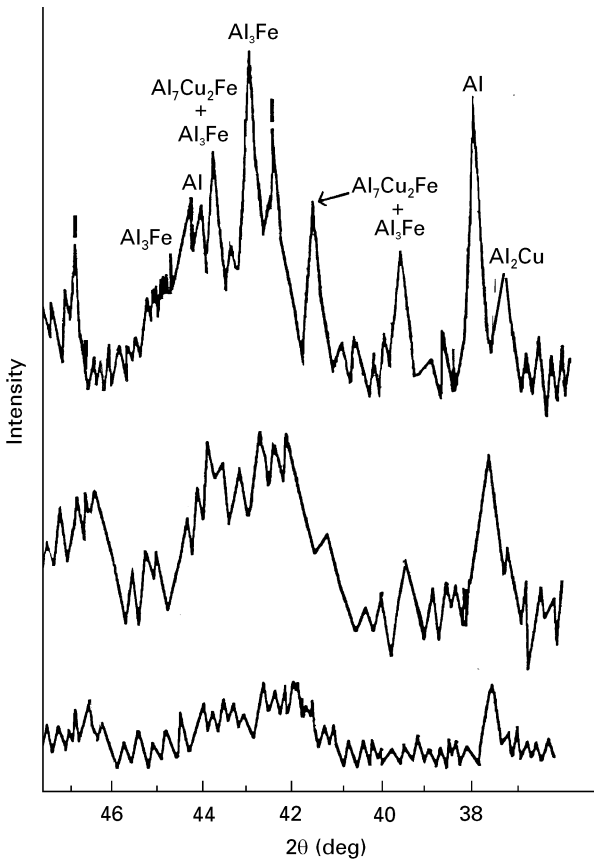

Figure 13 X-ray diffraction patterns from different regions in the wedge-shaped quaternary alloy 4 ($Al_{60}Fe_{15}Cu_{10}Cr_{10}$). The top spectrum corresponds to the thick region of the ingot, the spectrum in the middle to the medium region in the wedge ingot, and the bottom spectrum to the thin region of the wedge ingot.

Acknowledgements

The authors thank F. Solorio, J. G. Quezada (UMSNH) and J. L. Albarran, O. Flores, A. Gonzalez (UNAM), for technical help. G. Rosas thanks the UMSNH, U.A. Edo. Mor. and CONACYT for financial support.

References

1. A. P. TSAI, A. INOUE and T. MASUMOTO, *J. Mater Sci. Lett*. **6** (1987) 1403.
2. F. FAUDOT, A. QUIVY, Y. CALVAYRAC, D. GRATIAS and M. HAMERLIN, *Mater. Sci. Eng.* **A133** (1991) 383.
3. W. LIJUN, Z. LIHUA, X. JUEMIN, H. WANGYU, C. ZHENHUA and W. YUKUN, *Scripta Metall. Mater.* **32** (1995) 1325.
4. D. GRATIAS, Y. CALVAYRAC, J. DEVAUD-RZEPSKI, F. FAUDOT, M. HARMELIN, A. QUIVY and P. A. BANCEL, *J. Non-Cryst. Solids* **153**/**154** (1993) 482.
5. W. LIU and UWE KOSTER, *Z. Metallukde* **82** (1991) 10.
6. F. W. GAYLE, A. J. SHAPIRO, F. S. BIANCANIELLO and W. J. BOETTINGER, *Metall. Trans.* **23A** (1992) 2409.
7. Y. F. CHENG, M. J. HUI, X. S. CHEN and F. H. LI, *Philos. Mag. Lett*, **61** (1990) 173.
8. Z. ZHANG and N. C. LI, *Scripta Metall.* **24** (1990) 1329.
9. C. DONG, J. M. DUBOIS, M. de BOISSIEU and C. JANOT, *J. Phys. Condens. Matter* **2** (1990) 6339.
10. R. PEREZ, A. ARIZMENDI, J. A. JUAREZ-ISLAS and L. MARTINEZ, *J. Mater. Res* **8** (1993) 985.
11. A. J. BRADLEY and H. J. GOLDSCHMIDT, *J. Inst. Metals* **65** (1939) 389.
12. A. JHA, *Mater. Sci. Eng.* **A181**/**A182** (1994) 771.

Received 19 January
and accepted 31 July 1996